

Active and reactive energy management by renewables and BESS

Pradipta Kumar Nayak
College of Engineering Bhubaneswar, Odisha, India

Keywords: Renewable, Storage systems, Frequency and Voltage regulation, Remote communication absence.

Abstract

It can be increasingly interesting to employ a large amount of renewable energy in islanded systems; this is true for both the initial electrification of rural areas and the disconnection of some segments of the current distribution networks. To preserve frequency and voltage stability, an islanded system's many resources must be coordinated through a control approach. Unlike other studies, the authors have developed a method that can coordinate active and reactive producing output with storage system demands and features without requiring remote connections between various system locations. The control strategy modifies frequency and voltage to reduce power exchanges between the storage system and the network.

1 Introduction

Different issues are progressively enhancing the interest on off grid operation. On one hand, rural areas can be conveniently electrified through local autonomous systems, on the other one portions of distribution systems can be properly disconnected by the main grid, both in case of temporary faults or in case of scheduled maintenance activities. In both the contexts, renewables play a fundamental role. For rural or remote areas, the local electrification can be achieved avoiding issues mainly related to traditional generation unit powered by fossil fuel (petrol, diesel, etc.). For example, problems as reduced efficiency for low operational loading, noise and fossil fuel procurement, both in terms of availability and cost, can be dramatically reduced. In developed countries, local incentives have recently enhanced the economical interest in the renewable plants installation. With this increasingly diffusion of Distributed Generators (DGs), some portions of distribution networks are become active networks. Output power perturbation of these unpredictable sources (i.e. caused by cloud front or wind gusts) can be managed at different levels, investigating their impact on distribution level networks up to the interconnected transmission system.

Many research activities are investigating the autonomous operation of defined portions of distribution systems, enhancing supply continuity in case of network events. At present, looking to renewable technologies, solar and wind plants seem to present the most interesting characteristics, in particular in case of small installations: the primary source procurement absence (as regards to biomass plants), the installation easiness, almost negligible operational costs, scalable size plants and the recent drop in installation costs due to a rapid production capacity increase are important key driver for the diffusion of these technologies. In rural contexts, far away from the main grid, the traditional network electrification costs often overpass the local renewables installation investment. Therefore micro-grids or autonomous networks are becoming in those contexts a feasible choice for the electrification of depressed or remote areas.

The optimal management of autonomous networks locally compensates output power fluctuations in order to preserve the network stability and the supply quality. Aiming to intentionally minimize the use of fossil fuel generators (at least maintained as backup units), the role of a Battery Energy Storage System (BESS) can be strategic. In the short term, considering the low inertia of small isolated grid [1,2], a BESS can guarantee a proper voltage and frequency regulation due to its fast response. In the medium term, aiming to avoid a quick discharge of the storage system, a suitable energy management is required. In [3] a plant locally aggregating photovoltaic panels and batteries is introduced: the micro-grid is fed by controlling the internal State of Charge (SoC). Instead in the case of remote plants, communication links are considered unavoidable [1,4].

In this paper the authors present a control strategy involving both active and reactive power management of the connected plants (BESS and DGs). Differently from other approaches reported in literature, the proposed one does not make use of remote measures or communication systems between the different points of the network. This aspect allows the proposed strategy to be used also as backup controller in case of remote communications loss in traditional systems. In order to activate the desired behaviors in connected units, the BESS acts by modulating frequency and voltage at its Point of Common Coupling (PCC), according to its operational state, in particular the SoC of batteries.

2 Micro-grid control strategy

In interconnected networks the voltage vector is regulated in magnitude and frequency by the main grid. Several high power rotating generators, recently supported by DGs, face

variations in load requirements, also taking advantage of the statistical compensation between different loads.

Conversely, considering a micro-grid or an islanded portion of distribution network, e.g. caused by a fault event, a proper DG control scheme is necessary to regulate the voltage in magnitude and frequency. In fact, in case of small unbalances between generation and load, the frequency could freely vary while unsustainable voltage deviations could arise.

Different strategies can be used to regulate the voltage in an isolated system with several generators, both considering traditional rotating machines or inverter interfaced DGs. Generally the droop control is mainly used since it permits to avoid continuous communication links between the remote units. However this approach application is limited by specific drawbacks, e.g. the trade-off between power sharing and steady state voltage deviations both in magnitude and frequency [5,6]. To overpass this limit, secondary frequency control can be introduced. In order to coordinate the interactions between the DGs in regulating voltage, a master-slave approach or an overall supervisor sending proper signals to each DG has been developed [7,8].

In this work a control strategy for the management of isolated networks is proposed, aiming to correctly operate even in case of remote communications absence. A BESS, controlling voltage and frequency at its PCC (Vf unit), is interfaced with a controlled Voltage Source Inverter (VSI), which guarantees power balance management with quick dynamic performances. All the other connected plants, regulating active and reactive power injections, are current controlled as in grid tied applications.

In the long term point of view, the energy sustainability of the islanded system is preserved operating the BESS and DG units in a coordinated way. Each DG unit is called, within its energy availability and power capability, to modify its power injections to help the BESS in reducing the power exchanges with the network between defined thresholds, depending on SoC. The communication is achieved through small temporary deviations of the voltage vector imposed by the Vf unit at its PCC, both in magnitude and frequency. Therefore no explicit communication links or protocols are required.

In a previous work [9], authors developed the control strategy only focusing to the active power management. To enhance islanded network stability, this work introduces an improved strategy, involving also the reactive power management. The approach objective is the zeroing of the BESS reactive power exchange. In this way, the overall apparent power capability of the Vf inverter is available to face perturbations in load requirements or in DG generation output. Furthermore, reducing the current flowing in the BESS inverter, an increase in system efficiency can be obtained.

Vf unit control scheme

The Vf unit, composed by a BESS interfaced with a three-phase inverter operating in Pulse-Width Modulation (PWM) mode, acts as slack node ensuring voltage control at its PCC. The PWM modulation index P_{mi} is obtained through a Proportional-Integral (PI) controller aiming to follow a voltage set-point V_{ref} , as explained in Fig. 1 and in (1).

$$P_{mi} = K_{VP}(V_{ref} - V_B) + K_{VI} \int (V_{ref} - V_{BESS}) dt \quad (1)$$

While generally the voltage magnitude at the BESS PCC (V_{BESS}) is controlled at a fixed target value, in the proposed control strategy the set point V_{ref} strictly depends on the reactive power injected by the BESS into the grid. Aiming to involve DGs in locally compensating reactive power consumptions in order to nullify the BESS reactive exchange, the voltage at the BESS connection node is modulated around the rated value V_r . The voltage deviations imposed by the BESS modify the voltage profile along network feeders, stimulating the decentralized voltage regulation of DGs. All the DGs have to be equipped with local controller regulating their reactive power injections depending on the voltage at their PCC, as described below. The voltage reference V_{ref} reaches a steady-state value when BESS reactive power is zeroed.

To reach the target, the parameter V_{ref} is computed by a further PI controller elaborating the difference between $Q_{BESS,ref}$ and Q_{BESS} , as in (2).

$$V_{ref} = V_r + K_{Q,SS,ref} (Q_{BESS,ref} - Q_{BESS}) + K_{QI} \int (Q_{BESS,ref} - Q_{BESS}) dt \quad (2)$$

Measurement Q_{BESS} is obtained at the BESS PCC, while $Q_{BESS,ref}$ is set to zero in standard conditions. The reference parameter V_{ref} is limited in the range between V_{min} and V_{max} in order to avoid dangerous operating conditions in case generators are not able to modify their reactive power injections (or in case DGs are out of service).

As in [9], a frequency regulation strategy is also implemented to reduce the BESS active power flow, both in charging and discharging phases. Internal reference f_{ref} is evaluated making use of a $P_{BESS}-\Delta f$ droop. A stability dead-band, defined by $P_{BESS,f+}$ and $P_{BESS,f-}$, is introduced in order to preserve the system from frequency perturbations in case small variations in active power requirements happen. In case the BESS required active power P_{BESS} is between $P_{BESS,f-}$ and $P_{BESS,f+}$ thresholds, the micro-grid frequency is maintained at its reference value. When the BESS active power overpasses the $P_{BESS,f-}$ threshold, the frequency is reduced to involve the active power regulation of the connected DGs, according to the plot reported in Fig. 1. Dually, in case P_{BESS} overpasses the $P_{BESS,f+}$ threshold in charging phase, the frequency is increased to partially switch off the DGs. A further dead-band

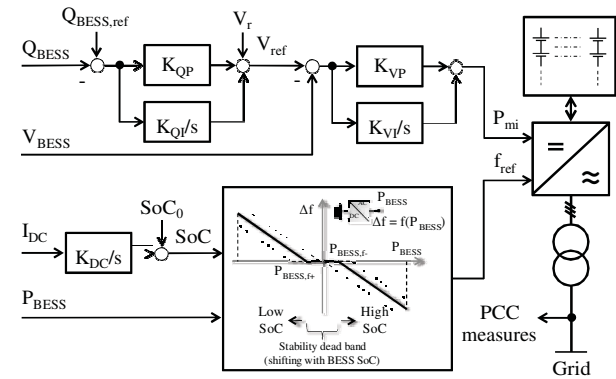


Fig. 1: Control scheme for the BESS Vf unit.

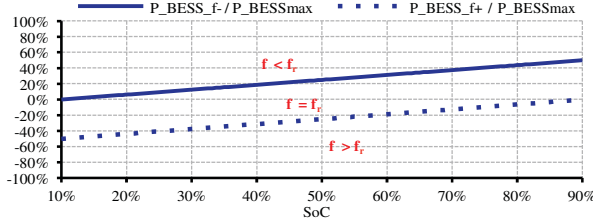


Fig. 2: Influence of batteries SoC on BESS active power dead-band limits.

ΔP is applied on thresholds $P_{\text{BESS},f+}$ and $P_{\text{BESS},f-}$ in order to avoid frequency perturbations when the system operates in proximity to one of these thresholds.

The dead-band limits directly depend on storage system SoC as described in Fig. 2, so the BESS admitted active injection is greater in case the internal SoC is high, while the BESS immediately requires the contribution of DGs in case a load increase involves the BESS discharging phase from a low SoC condition.

The storage system is represented by means of its capacity and a simplified SoC calculation algorithm based on Coulomb counting method [10,11], as reported in Fig. 1. Batteries dynamic behaviour has not been investigated since the proposed strategy involves slow variation in the BESS operating conditions, while typical batteries reaction times are extremely shorter.

DG units control scheme

All the DG units work basically as in grid-connected systems, allowing active and reactive power modulation depending on frequency and voltage measurements at their PCCs respectively. Even if different DG technologies, e.g. rotating machines, are compatible with the proposed strategy, in this work a current controlled VSI is considered for each DG, as described in Fig. 3. A Phase Locked Loop (PLL) device calculates the phase angle θ of the voltage vector to synchronize the inverter with the grid voltage, as sustained from the Vf unit. The phase angle is sent to the control scheme for the Park transformation. Generally DG units equipped with inverters are interfaced with the grid through large filter inductors (LC or LCL filters) and in some cases also transformers. Thus the physical interfacing impedance is often predominantly inductive, so the active power control through the direct axis current I_d and the reactive power control through the quadrature axis current I_q are justified. However the effective output impedance of the inverter can be also influenced by the control scheme, introducing virtual inductors [12]. In this work, inductive impedance is assumed. Making use of DC quantities in d-q axes allows controlling the inverter dynamics through simple PI regulators. The reference values of direct and quadrature currents ($I_{d,\text{ref}}$ and $I_{q,\text{ref}}$ respectively) are obtained through PI controllers, which use the active and reactive power references P_{ref} and Q_{ref} . As summarized in (3), the set-point P_{ref} consists of three parts: the initial value P_0 ; a proportional component obtained with a P- Δf droop, defining as Δf the difference between the measured frequency f and the rated value f_r ; a third

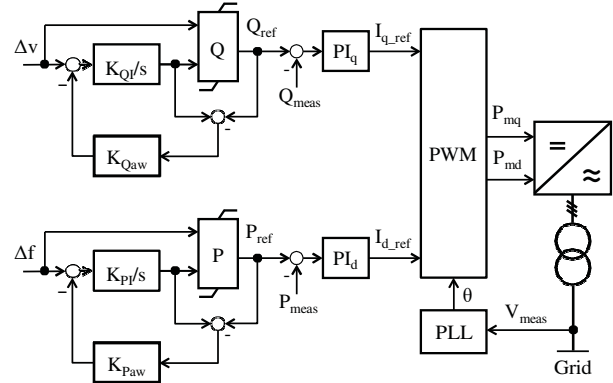


Fig. 3: Control scheme for the DG units.

component obtained by integrating the frequency deviation Δf .

$$P_{\text{ref}} = P_0 + m_p(f_r - f) + k_{I,P} \int (f_r - f) dt \quad (3)$$

The active power set-point is therefore dependent on the frequency deviation imposed by the BESS unit. In case the DG makes use of an unpredictable renewable source, during under-frequency transitions the active power will be increased only if further energy is locally available.

Similarly, the reference value of reactive power Q_{ref} is composed by two terms: a Q- Δv droop term and an integrative term, as described in (4). Variation Δv is defined as the difference between the measured voltage v at the DG PCC and the rated value v_r .

$$Q_{\text{ref}} = -(\ + k_{I,Q}) \int (v_r - v) dt \quad (6)$$

Two anti-wind-up schemes, represented in Fig. 3 with K_{Qaw} and K_{Paw} , are introduced in order to prevent the integration of voltage and frequency errors in case the controllers are saturated.

3 Case study

A realistic radial structure distribution network has been modelled to demonstrate the proposed approach effectiveness. DG output, BESS operating conditions and frequency/voltage trends are studied and reported in the figures below. Simulations have been carried out in DIgSILENT PowerFactory environment, while results are exported and post processed making use of MS Excel.

Two Medium Voltage (MV) feeders ($V_n = 20$ kV) compose the case study network, as represented in Fig. 4. Each branch is sized in order to assure a maximum admitted loading of 80% in every network operating condition, both considering the passive arrangement and the configuration with the maximum DG penetration level. Furthermore the feeder is designed to guarantee a maximum voltage drop in passive configuration equal to 4%.

In order to better test the control strategy, the main characteristics of the feeders widely differ. The lower one in Fig. 4 (feeder A, from node 1 to node 5) is quite long (20

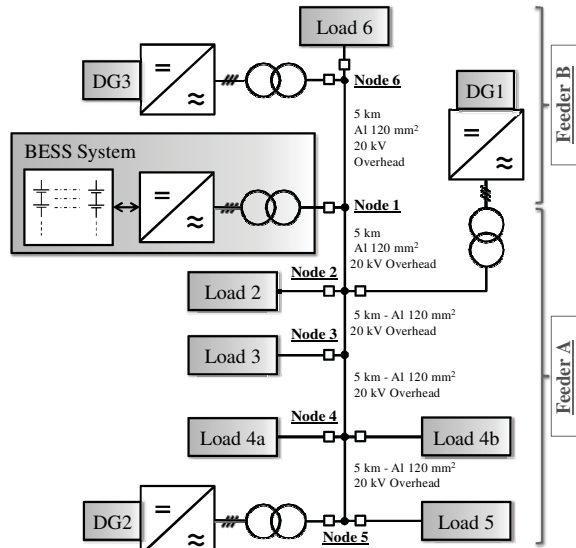


Fig. 4: MV islanded network case study.

km), multiple loads are connected at each node for an overall amount of 1.47 MW (power factor 0.92), a couple of generators are connected in the first busbar (node 2) and in the most peripheral one (node 5). Oppositely, the upper feeder (feeder B) is quite short (5 km) and the generated power widely overpasses the local load in standard conditions, so the active

power flows from the feeder to the common busbar (node 1). All the branches are modelled as overhead lines, with aluminium conductors and equivalent longitudinal impedance equal to $(0.25 + j 0.345) \Omega$. Each load is represented asohmic-inductive impedance, so effective active and reactive power absorptions strictly depend on the voltage and the frequency at the connection node.

DG units have rated power equal to 1.0 MW, even if active and reactive injections are called to respond to local frequency and voltage measurements at their PCCs, as reported in the upper section. In the proposed case study, each DG is interfaced with the network through an electronic power converter, even if the control strategy is easily applicable to every DG technology with minor adjustments. DG can inject into the grid active power and inductive

Event #	Time t (s)	Event short description
a)	4.0	Load 5 disconnection (feeder A overall load decreases of 0.41 MW – 0.17 Mvar)
b)	8.0	Load 4b disconnection (feeder A overall load decreases of 0.69 MW – 0.30 Mvar)
c)	12.0	Load 5 connection (feeder A overall load increases of 0.41 MW – 0.17 Mvar)
d)	16.0	Load 4b connection (feeder A overall load increases of 0.69 MW – 0.30 Mvar)
e)	20.0	DG2 disconnection (feeder A becomes passive from DG1 PCC to the end node)

Table 1: Simulation events.

reactive power.

A BESS unit is connected at node 1, with a rated capacity of 1.0 MWh, SoC operating in the range 10÷90% and minimum admitted discharge duration equal to 0.8 hour, which means maximum power in discharging phase equal to 1.0 MW. The same constraint is considered in the charging phase.

Even if the simulation time is limited to 26 s, several stressful network operation conditions are exploited. Multiple events are introduced with the scope of severely verifying the control strategy performances in guaranteeing frequency and voltage regulation between admitted thresholds. Events are represented as connections and disconnections of loads or DG units, as briefly described in Table 1. Due to the discontinuous events, a quick transition can be appreciated immediately after the network perturbation. In the following phase, the BESS reacts modifying frequency and voltage at the node 1 in order to progressively reach the subsequent steady state condition.

Fig. 5 reports the overall load supplied by the islanded network. A medium load disconnection and a high load outage are clearly identified as the first two events.

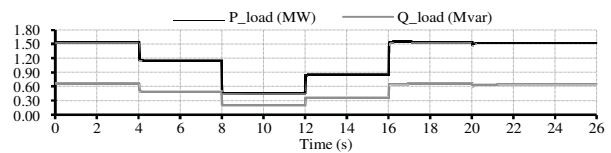


Fig. 5: Islanded network overall load.

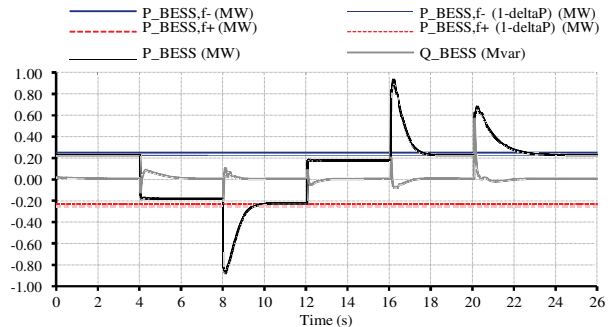


Fig. 6: BESS active and reactive injections.

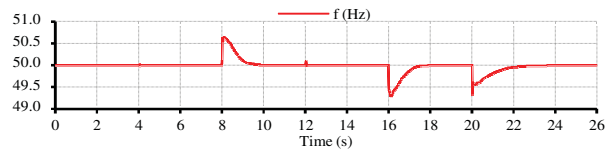


Fig. 7: Network frequency behaviour.

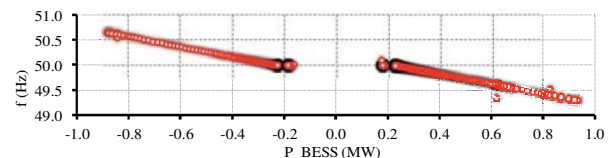


Fig. 8: BESS operation equivalent representation on a power-frequency plan

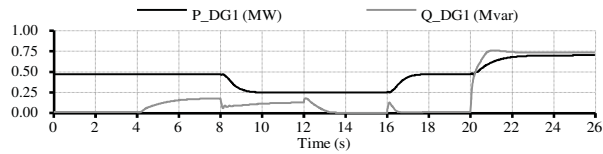


Fig. 9: DG1 active and reactive power injections.

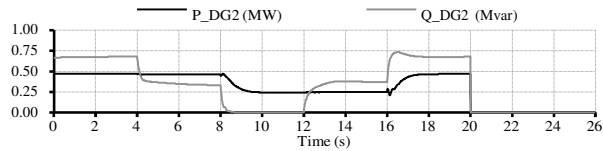


Fig. 10: DG2 active and reactive power injections.

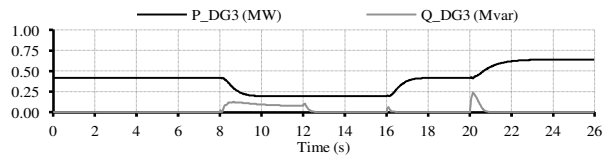


Fig. 11: DG3 active and reactive power injections.

Subsequently, the same loads are re-connected to the system in the third and fourth events. DG2 disconnection impacts on the active and reactive overall load requirements due to the frequency and voltage perturbations introduced by the event. BESS active and reactive power injections are reported in Fig. 6. Considering active power, the figure reports the admitted dead-band amplitude, within which the BESS exchanges active power not forcing a frequency variation, i.e. not requiring DG modulation. Since admitted dead band strictly depends on batteries SoC, an initial SoC of 50% is set in the simulation, which means a symmetrical admitted dead-band as regards to the horizontal axis. Due to the short duration of the simulation, SoC varies for an extremely low percentage, not appreciably impacting on dead-band thresholds. It is possible to see that events a) and c) are fully compensated by the BESS in terms of active power, since the BESS active exchange remains between the admitted dead band for reduced load variations. As a consequence, frequency is maintained at its rated value, even if small perturbations due to load events are appreciable at $t = 4$ s and $t = 12$ s, as shown in Fig. 7. Differently, large network perturbations, e.g. large load connection/disconnection or DG outage, induce the BESS to require DG support aiming to maintain its exchanged active power between the admitted values. As a consequence, an over-frequency transition is introduced by the BESS at $t = 8$ s to require the output reduction of DGs, while under-frequency transitions are imposed to front both the load connection in $t = 16$ s and the subsequent generation outage in $t = 20$ s.

Fig. 8 reports the BESS operation conditions in the overall simulation, in terms of active power exchanged with the network compared with the imposed frequency: excluding some points representing the quick dynamic responses to discontinuous events, it is possible to clearly identify the admitted dead-band in terms of active power, the regulation

slope in the power-frequency plan and the steady-state conditions, represented as dark shadowed points.

Considering the reactive power exchange between the storage system and the network, the BESS action on local voltage regulation is able to involve the DG in completely compensate the load requirements and the network losses in all the steady-state regimes following each event. In this way, BESS reactive power injections is controlled to zero after the transition phase, so all the BESS capability can be available to compensate network perturbations, guaranteeing the highest stability level to the islanded system.

In Fig. 9, Fig. 10 and Fig. 11 the behaviours of the DG units can be compared, considering that each generator controller has been set with the same parameter calibration. The active power behaviours are homothetic, since all the DG units have the same rated power and the frequency is roughly the same at each of their PCCs. Differently, since the reactive power regulation is influenced by the local measured voltage, only DG2 is called to inject reactive power into the grid in the first section of the simulation, since it is connected on the end node of the feeder presenting the larger load requirements. The disconnection of peripheral loads in feeder A, which means that active power flows from the ending busbar (node 5) to BESS, induces a partial contribution of DG1 in compensating reactive power requirements. The second load disconnection in $t = 8$ s imposes a contribution in terms of reactive power also to DG3, since feeder A and feeder B behaviours becomes similar in terms of active power exchanged with node 1. The feeder A loads re-connection and the further DG2 disconnection in $t = 20$ s bring back the feeder A to a passive condition in terms of active power exchanges with the BESS, so feeder A DGs are called to supply all the network reactive power consumption, DG2 in a first time and later DG1 as a consequence of DG2 outage.

Voltage trends at each PCC are reported in Fig. 12. In case all the DGs are connected to the network, the control strategy

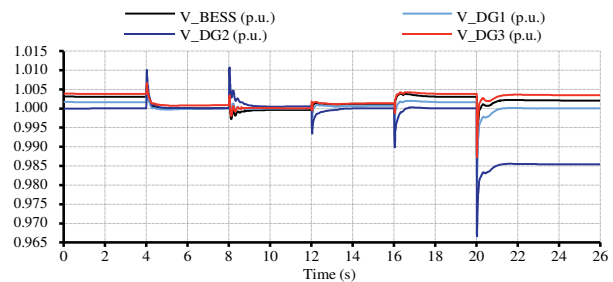


Fig. 12: Voltage trends at the PCCs

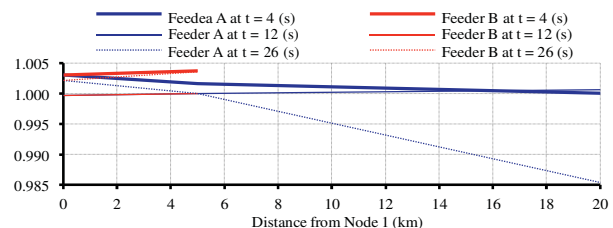


Fig. 13: Voltage profiles of network feeders for three simulation times.

indirectly induces the lowest PCC voltage to be regulated to the rated voltage. In this way, the DGs connected to the more passive feeder are called to proportionally generate the overall reactive consumption of the islanded system. In case a DG is disconnected, the other ones' lowest PCC voltage is controlled to the rated value, while the line branch sizing criterion guarantees the minimum admitted voltage value in the end nodes. Fig. 13 represents the feeder voltage profiles for different simulation times, underlining the large variations in feeder A operating conditions, particularly after DG2 outage. At the same time, the voltage level set from the BESS controller, depending on its reactive power exchange, is clearly visible for the selected instants. With the aim to reduce the BESS reactive power exchange, the voltage at the storage system PCC is regulated lower than the rated value in charging phase steady-state regime, while it is set higher than 1 p.u. when the first and the last steady-state conditions are reached by the system.

4 Conclusions

A novel control strategy addressed to optimally manage both active and reactive power flow in an islanded network has been implemented. In particular, by controlling the reactive power exchange between the storage system and the network, the BESS capability is maintained fully available to compensate load or generation events, guaranteeing the system frequency and voltage stability. Furthermore, the approach preserves the storage system from an accelerated ageing due to a high number of charge-discharge cycles.

The developed strategy is also able to improve the voltage profiles of the islanded network, by inducing the most peripheral DG units to generate the overall reactive power requirement depending on the voltage at their connection nodes.

Islanded network stability is assured without use of remote communications between different points of the system. This allows the complete management of extended systems in which remote connections are missing or temporarily out of service.

Simulations results demonstrate the approach effectiveness in terms of frequency-voltage stability and in coordinating different resources interfaced with the network, also in case the relevant connection nodes are quite distant.

References

- [1] J.Y. Kim, J.H. Jeon, S.K. Kim, C. Cho, J.H. Park, H.M. Kim, K.Y. Nam, "Cooperative Control Strategy of Energy Storage System and Microsources for Stabilizing the Microgrid during Islanded Operation", *Power Electronics, IEEE Transactions on*, vol. 25, no. 12, pp. 3037-3048, (December 2010).
- [2] M.J. Erickson, R.H. Lasseter, "Integration of battery energy storage element in a CERTS microgrid", *Energy Conversion Congress and Exposition (ECCE), 2010 IEEE*, pp. 2570-2577, (12-16th September 2010).
- [3] Y. Zhang, H.J. Jia, L. Guo, "Energy management strategy of islanded microgrid based on power flow control", *Innovative Smart Grid Technologies (ISGT), 2012 IEEE PES*, pp. 1-8, (16-20th January 2012).
- [4] Y. Zhu, F. Zhuo, L. Xiong, "Communication platform for energy management system in a master-slave control structure microgrid", *Power Electronics and Motion Control Conference (IPEMC), 2012 7th International*, vol. 1, pp. 141-145, (2-5th June 2012).
- [5] J.M. Guerrero, L.G. de Vicuna, J. Matas, M. Castilla, J. Miret, "A wireless controller to enhance dynamic performance of parallel inverters in distributed generation systems", *Power Electronics, IEEE Transactions on*, vol. 19, no. 5, pp. 1205-1213, (September 2004).
- [6] A. Tuladhar, K. Jin, T. Unger, K. Mauch, "Parallel operation of single phase inverter modules with no control interconnections", *Applied Power Electronics Conference and Exposition, 1997, APEC '97 Conference Proceedings 1997, Twelfth Annual*, vol. 1, pp. 94-100, (23-27th February 1997).
- [7] J.M. Guerrero, J.C. Vasquez, J. Matas, M. Castilla, L.G. de Vicuna, "Control Strategy for Flexible Microgrid Based on Parallel Line-Interactive UPS Systems", *Industrial Electronics, IEEE Transactions on*, vol. 56, no. 3, pp. 726-736, (March 2009).
- [8] F. Katiraei, M.R. Iravani, "Power Management Strategies for a Microgrid With Multiple Distributed Generation Units", *Power Systems, IEEE Transactions on*, vol. 21, no. 4, pp. 1821-1831, (November 2006).
- [9] F. Bignucolo, A. Raciti, R. Caldon, "A control strategy for the management of islanded networks with renewables and storage systems", *UPEC 2014, 49th Universities' Power Engineering Conference*, Cluj-Napoca, (2-5th September 2014).
- [10] M. Coleman, C.K. Lee, C. Zhu and W.G. Hurley, "State-of-Charge Determination From EMF Voltage Estimation: Using Impedance, Terminal Voltage, and Current for Lead-Acid and Lithium-Ion Batteries," *Industrial Electronics, IEEE Transactions on*, vol. 54, no. 5, pp. 2550-2557, (October 2007).
- [11] Z. Miao, L. Xu, V.R. Disfani and L. Fan, "An SOC-Based Battery Management System for Microgrids," *Smart Grid, IEEE Transactions on*, vol. 5, no. 2, pp. 966-973, (March 2014).
- [12] W. Yao, M. Chen, J. Matas, J.M. Guerrero, Z.M. Qian, "Design and Analysis of the Droop Control Method for Parallel Inverters Considering the Impact of the Complex Impedance on the Power Sharing," *Industrial Electronics, IEEE Transactions on*, vol. 58, no. 2, pp. 576-588, (February 2011).